

SUPPORTING INFORMATION
MRI Sensing Based on Displacement of Paramagnetic Ions
from Chelated Complexes

Tatjana Atanasijevic, Xiao-an Zhang, Stephen J. Lippard, and Alan Jasanoff

Table of Contents	page
1. Experimental section	S2
2. Supplemental references	S4
3. Suppl. Fig. 1: Relaxation rates in control conditions	S5
4. Suppl. Fig. 2: Calcium dependence of relaxivity ratios	S6
5. Suppl. Fig. 3: Modeling of inner sphere relaxation changes for Mn ₄ CaM	S7
6. Suppl. Fig. 4: T_1 changes in the presence of competitor ions	S8
7. Suppl. Fig. 5: T_2 changes in the presence of competitor ions	S9

EXPERIMENTAL SECTION

Binding and competition assays. Chemicals were purchased from Sigma-Aldrich (St. Louis, MO). Chloride salts of Mn^{2+} , Ca^{2+} , Zn^{2+} , Mg^{2+} , and K^+ were used, along with Na_4EGTA and Na_4BAPTA . Hexahistidine-tagged *Xenopus laevis* CaM E104Q was purified by nickel affinity chromatography (Qiagen, Valencia, CA) from *E. coli*, as described previously.^[1] All solutions were formulated in MOPS buffer (30 mM 3-(*N*-morpholino)propanesulfonic acid, pH = 7.2) or artificial cerebrospinal fluid (150 mM NaCl, 3 mM KCl, 0.8 mM MgCl_2 , 0.8 mM Na_2HPO_4 , 0.02 mM NaH_2PO_4 , pH = 7.4).

Magnetic resonance imaging and analysis. Mixtures prepared as described above were arrayed into 384-well microtiter plates (80 μL /well) modified to fit into a 9 cm birdcage resonator probe (Bruker Instruments, Billerica, MA). Probe and sample were positioned within a 40 cm bore Magnex 4.7 T magnet equipped with Bruker 12 cm inner-diameter gradients (26 G/cm maximum) and scanned at room temperature (22 °C) using a 200 MHz Avance console running Paravision 3.0 (Bruker Instruments). Images were acquired using a multi-echo spin echo pulse sequence, with repetition times ranging from 0.1-5.0 s and echo times from 10-320 ms, across a 2 mm horizontal slice positioned to transect the middle of each microtiter well (in-plane resolution 0.47 mm, field of view 60 x 60 mm, 1-16 echos). Data were analyzed offline using custom routines implemented in Matlab (Mathworks, Natick, MA). Relaxation times were obtained by fitting monoexponential decay functions to image intensities averaged over each microtiter well; relaxivities were calculated using the known sample concentrations. Where shown throughout the text, error margins represent standard errors of the mean of multiple measurements. Data visualization and additional numerical analysis were performed with KaleidaGraph (Synergy Software, Reading, PA). These procedures included fitting of CaM titration data to the binding equation $\Theta = [\text{Ca}^{2+}]^n / (\text{EC}_{50} + [\text{Ca}^{2+}]^n)$,

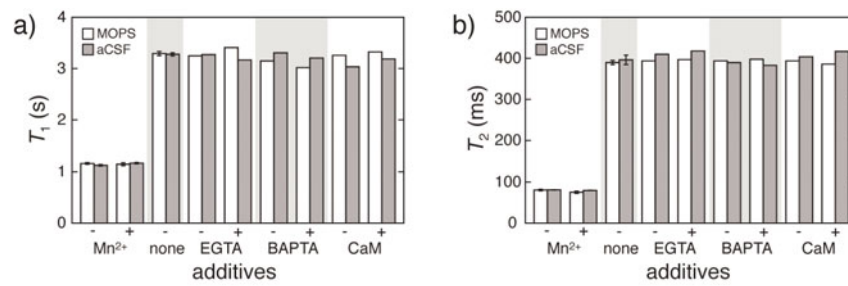
where Θ is the fractional relaxivity change, n is the Hill coefficient, and EC_{50} is the transition midpoint. Involvement of the CaM histidine tag in relaxivity changes was excluded by performing a calcium titration on 25 μM hexahistidine-tagged ubiquitin (Sigma-Aldrich) in the presence of 100 μM MnCl_2 . Values of r_1 and r_2 showed no noticeable $[\text{Ca}^{2+}]$ dependence in a range from 0-20 mM, and the presence or absence of the tagged protein did not significantly alter the relaxation rates recorded from 100 μM Mn^{2+} .

Relaxivity modeling. For comparison with experimental results, inner sphere longitudinal relaxivities of Mn_4CaM and Mn^{2+} (aq) at 4.7 T and 22 °C were estimated using the Solomon-Bloembergen-Morgan equations.^[2-4] Calculations were performed in Matlab with a Mn^{2+} -proton distance $r = 2.9 \text{ \AA}$,^[5] hyperfine coupling constant $A/h = 1 \text{ MHz}$,^[4] and electronic relaxation time T_{1e} fixed at 2 μs .^[6] Values of r_1/q were computed over a range of τ_M and τ_R values. Specific estimates for the τ_M and τ_R of Mn^{2+} (aq) and Mn_4CaM were obtained from literature sources: for Mn^{2+} (aq) $\tau_M = 50 \text{ ns}$ ^[7] and $\tau_R = 30 \text{ ps}$ ^[8] were assumed, and for Mn_4CaM $\tau_M = 2.3 \text{ ns}$ (from Mn-EDTA^[9]) and $\tau_R = 12 \text{ ns}$ (from apo-CaM^[10]) were estimated. Qualitative features of the modeling results persisted under reasonable variation of the estimated parameters. The crystal structure of calbindin loop 2 in complex with Mn^{2+} (Fig. 1c)⁴ suggests by analogy that each Mn^{2+} -bound EF hand of CaM will have $q = 2$. Ca^{2+} ions complexed to CaM or calbindin loop 2 each coordinate one water molecule only.^[11, 12]

SUPPLEMENTAL REFERENCES

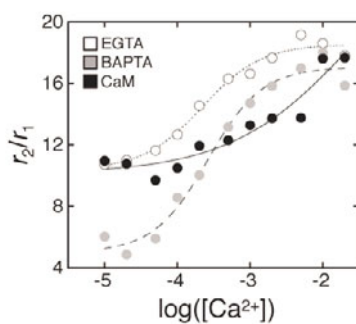
- [1] T. Atanasijevic, A. Jasanoff, *Nat Protoc* **2007**, 2, 2582.
- [2] I. Solomon, *Phys. Rev.* **1955**, 99, 559.
- [3] N. J. Bloembergen, *J. Chem. Phys.* **1957**, 27, 572.
- [4] N. Bloembergen, L. O. Morgan, *J. Chem. Phys.* **1961**, 34, 842.
- [5] S. Richards, B. Pedersen, J. V. Silverton, J. L. Hoard, *Inorg Chem* **1964**, 3, 27.
- [6] J. S. Troughton, M. T. Greenfield, J. M. Greenwood, S. Dumas, A. J. Wiethoff, J. Wang, M. Spiller, T. J. McMurry, P. Caravan, *Inorg Chem* **2004**, 43, 6313.
- [7] T. J. Swift, R. E. Connick, *J. Chem. Phys.* **1962**, 37, 307.
- [8] P. Caravan, C. T. Farrar, L. Frullano, R. Uppal, *Contrast Media Mol Imaging* **2009**, 4, 89.
- [9] D. W. Margerum, G. R. Cayley, D. C. Weatherburn, G. K. Pagenkopf, in *Coordination Chemistry, Vol. 2* (Ed.: A. E. Martell), American Chemical Society, Washington, DC, **1978**, pp. 1.
- [10] N. Tjandra, H. Kuboniwa, H. Ren, A. Bax, *Eur J Biochem* **1995**, 230, 1014.
- [11] R. Chattopadhyaya, W. E. Meador, A. R. Means, F. A. Quioco, *J Mol Biol* **1992**, 228, 1177.
- [12] M. Andersson, A. Malmendal, S. Linse, I. Ivarsson, S. Forsen, L. A. Svensson, *Protein Sci* **1997**, 6, 1139.

Supplementary Figure 1



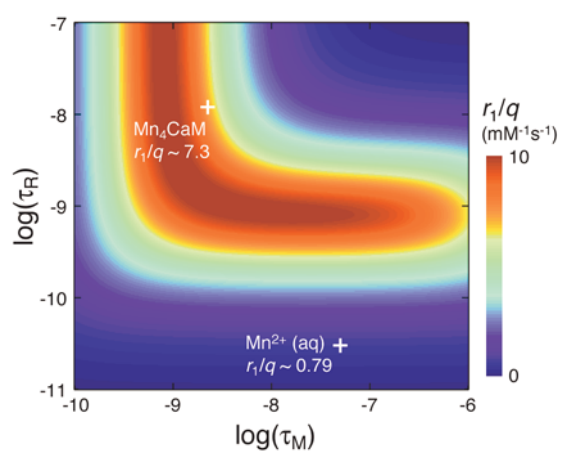
Supplementary Figure 1. a) T_1 and b) T_2 values recorded from control samples lacking (-) or containing (+) 1 mM CaCl₂, and other additives noted. Additive concentrations were 100 μ M for Mn²⁺, EGTA, and BAPTA, and 25 μ M for CaM. Samples were formulated in 30 mM MOPS buffer (white bars) or aCSF (gray bars). Standard errors of the mean indicated for samples where multiple measurements were made ($n = 2-3$).

Supplementary Figure 2



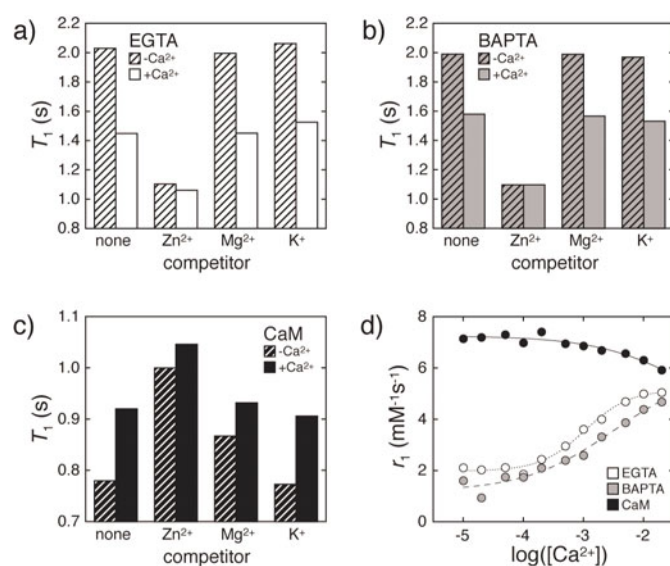
Supplementary Figure 2. Graphs of the T_2 to T_1 relaxivity ratio (r_2/r_1) as a function of calcium concentration for EGTA (open circles), BAPTA (gray circles), and CaM (black circles); data are equivalent to those in Fig. 2 of the main text. All three ligands display substantial r_2/r_1 changes over the calcium range investigated (most pronounced for BAPTA), indicating the possibility of ratiometric $[\text{Ca}^{2+}]$ determination using Mn^{2+} displacement-based agents.

Supplementary Figure 3



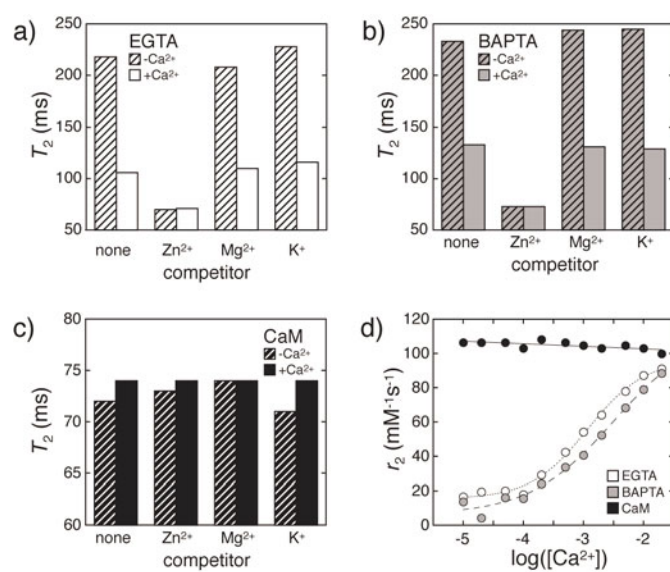
Supplementary Figure 3. Inner sphere longitudinal relaxivity per bound water molecule (r_1/q) computed from the Solomon-Bloembergen-Morgan equations, using parameters chosen to approximate behavior of $S = 5/2$ Mn^{2+} complexes at 4.7 T and 22 °C. Rotational and water exchange time constants (τ_R and τ_M) span ranges including reasonable estimates for Mn_4CaM and $\text{Mn}^{2+}(\text{aq})$ (combinations marked by white crosses); additional parameters were fixed, as described in the experimental section. The calculated r_1/q values predict that Mn_4CaM with $q = 1$ or 2 would display significantly greater relaxivity than $\text{Mn}^{2+}(\text{aq})$, as was observed experimentally.

Supplementary Figure 4



Supplementary Figure 4. Calcium-dependent T_1 changes recorded from 100 μM Mn²⁺ mixtures with a) 100 μM EGTA, b) 100 μM BAPTA, or c) 25 μM CaM, in the absence or presence of competing diamagnetic cations (each 1 mM), and in the absence (striped bars) or presence (solid bars) of 1 mM Ca²⁺. d) Titration of Ca²⁺ against Mn-EGTA, Mn-BAPTA, or Mn₄CaM in artificial cerebrospinal fluid, showing effects of biomimetic ion concentrations on titration curves. Mn²⁺, Ca²⁺, and binding ligand concentrations as in main text Fig. 2b. Note that 1 mM Ca²⁺ did not bring about maximal relaxivity changes for any of the ligands. 1 mM Zn²⁺ was more effective at displacing Mn²⁺ than 1 mM Ca²⁺, and therefore resulted in larger relaxation changes for all three chelators. The biologically relevant competitors Mg²⁺ and K⁺ did not alter calcium responses observed for Mn-EGTA and Mn-BAPTA, however, and Mg²⁺ only partially attenuated the Mn₄CaM response to 1 mM Ca²⁺.

Supplementary Figure 5



Supplementary Figure 5. T_2 values measured from samples containing a) Mn-EGTA, b) Mn-BAPTA, and c) Mn₄CaM, each in the absence (striped bars) or presence (solid bars) of 1 mM Ca²⁺ and designated competitor ions (1 mM), and corresponding to the T_1 measurements presented in Supplemental Fig. 4. d) Titration curves of r_2 vs. calcium concentration for mixtures containing 100 μ M Mn²⁺ with equimolar EGTA (open circles), BAPTA (gray circles), or 25 μ M CaM (black circles).